Solid-state supercapacitors for electronic device applications

Liping Ma and Yang Yang[a)]
Department of Materials Science and Engineering, University of California Los Angeles, Los Angeles, California 90095

(Received 26 May 2005; accepted 27 July 2005; published online 13 September 2005)

We report an all-solid-state supercapacitor with device fabrication by a simple vacuum thermal evaporation method, which allows not only a multilayer stacking structure to further enhance the capacitance, but also permits the supercapacitor to be easily incorporated with other electronic devices, showing interesting characteristics for both fundamental study and practical applications. Discussions about the mechanism of the supercapacitor is given. © *2005 American Institute of Physics*. [DOI: 10.1063/1.2051797]

Electric double-layer capacitors (EDLCs, or electrochemical supercapacitors),[1] originally consisting of liquid electrolytes, have been widely regarded as energy storage devices for memory backup systems that can provide power during the temporary failures of primary power sources. Recently, all-solid-state supercapacitors have generated much attention.[2–5] Carbon materials, such as activated carbons,[6] carbon fibers,[7] carbon aerogels,[8] and carbon nanotubes[9] have been used as EDLC electrodes because of their high surface area. The carbons electrodes may be formed by carbonization of polymers,[10] or prepared as pellets by pressing a mixture containing carbons and binder.[5] Solid-state electrolytes,[5] such as yttria-stablized zirconia composite,[2] organic-inorganic nanocomposite materials,[4] and Nafion®-based polymers,[5] were used for the formation of all-solid-state supercapacitors. The formation of the solid-state supercapacitors reported up to date involves solution processing, high-pressure pressing, high-temperature sintering, and sputtering techniques. The polymer membrane and electrode assembly was generally obtained by contacting face to face membrane and electrode pressing.[5]

In addition to the application of energy storage devices, supercapacitors may also be used as building block in electronic devices, where small dimensions and ease of fabrication are required in order to be incorporated with other electronic cells. In this letter, we report the formation of supercapacitors by a simple thermal evaporation method, which is ideal in combination with organic electronic devices such as organic diodes,[11] organic light-emitting diodes,[12] and organic memory devices.[13] The high density of storage charges of the supercapacitor cell may have effects on its associated active cell and exhibit interesting phenomenon.[14] This opens a way for new electronic devices and their applications.

The capacitor structure we studied here is the same as the traditional capacitor, with a dielectric layer sandwiched between two electrodes as shown in the top-right inset of Fig. 1. The dielectric material used here is lithium fluoride (LiF), and the electrode materials may be gold (Au), aluminum (Al), and copper (Cu). In the letter, we focus on using Cu for both the top and bottom electrodes since Al may have some chemical reaction with LiF and may cause device degradation.[15]

Vacuum thermal evaporation methods were used for device fabrication. Materials were purchased from Aldrich and they were used as received. Cu was first deposited on a precleaned glass substrate as the bottom electrode, followed by the LiF layer and the top electrode layer. The device area was definied by the crossover between the top and bottom electrodes. During deposition the chamber vacuum was approximately 1×10^{-6} Torr. All the deposited layers were finished in sequence without breaking the chamber vacuum. The capacitance of the devices were measured by using an HP 4284A precision LCR meter. The transient charging measurement was done by using an HP 214B pulse generator and a TDS 460 oscilloscope. The surface morphology of both the electrode and LiF layer were measured using atomic force microscopy (AFM). The relative humidity (RH) dependence of device capacitance was controlled and measured by introducing water vapor in an environmental chamber using pure nitrogen gas as the carrier. All the measurements were done at room temperature.

The capacitance of our devices turns out to be unexpectedly higher than regular capacitors, and shows strong RH dependence. Figure 1 shows the frequency dependence of the device-specific capacitance with 30 mV detecting ac voltage under RHs of 34% and 80%, respectively. It can be seen from Fig. 1 that the specific capacitance for the device mea-

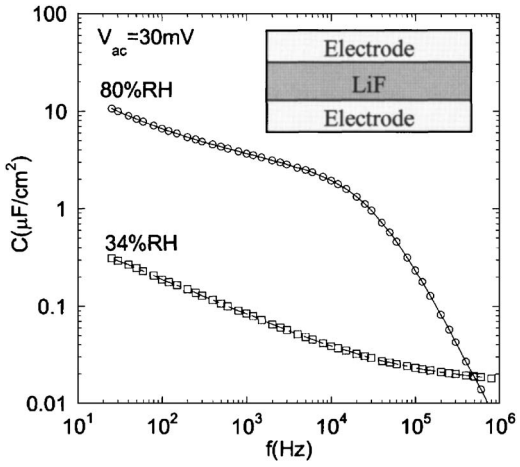

FIG. 1. Frequency-dependent specific capacitance for a Cu/LiF/Cu capacitor measured at relative humidities of 34% and 80%, respectively.

[a)]Author to whom correspondence should be addressed; electronic mail: yangy@ucla.edu

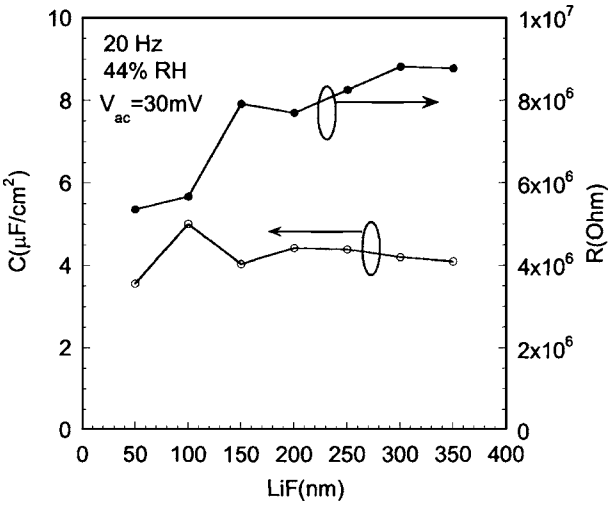

FIG. 2. LiF-thickness dependence of device capacitance and resistance measured at 44% RH and room temperature without dc bias.

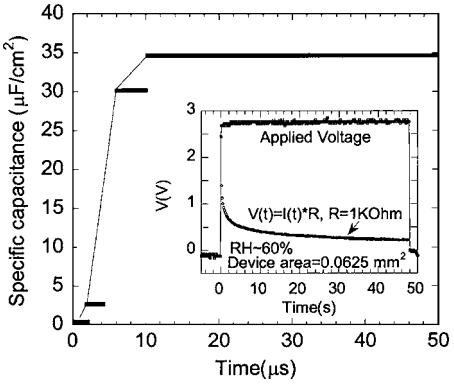

FIG. 3. The capacitance response to the applied voltage pulse. The inset shows the device current response to an applied voltage pulse. The capacitance, at various time windows, is obtained by fitting the charging current at various time ranges (0–2, 2–4, 4–10, and 10–50 μs) using $I=I_a \exp(-t/RC)+I_o$, where $R=1$ kΩ; I_a, I_o, and C (device capacitance, assuming it is constant in a given time range) are the fitting parameters.

sured at 80% RH is about 1.5 orders in magnitude higher than that measured at 34%. The specific capacitance measured at 80% RH at 25 Hz is about 10 μF/cm^2, which is about 400 times higher than a regular LiF capacitor (taking the dielectric constant of LiF as 9 and the thickness of the LiF layer is 320 nm, the specific capacitance of a regular LiF capacitor is about 0.025 μF/cm^2). It can also be seen from Fig. 1 that the capacitance of the device is frequency dependent. At a frequency above 10 kHz, the capacitance decreases tremendously, indicating that the capacitor's speed is around 10 kHz under 30 mV ac detecting voltage bias and possibly ion transport within the device limits the speed. It should be noted that when dc bias is applied to the capacitor, the capacitance of the device usually increases considerably, leading to a specific capacitance of the capacitor in the range of tens of μF/cm^2, which is typical for electrochemical supercapacitors.[1]

We also varied the thickness of the LiF layer from 50 to 350 nm during device fabrication, and found that both the capacitance and the resistance of the device show a very weak relationship with the LiF thickness (in 150–350 nm thickness range, Fig. 2). Therefore, the huge capacitance must come from the interfaces of the devices rather than, as in a regular capacitor, being related to the materials dielectric constant and film thickness. It should be mentioned that when the LiF thickness is below 50 nm, the capacitor may be subject to electrical shorts because of Cu diffusion. In addition, we did not put a separator within the LiF layer, which leads to the supercapacitor having leakage current in the nano- to microampere range.

The speed of capacitor is an important parameter for both fundamental study and applications. The frequency dependence of the device capacitance shown in Fig. 1 indicates that our capacitor speed under 30 mV ac detecting voltage condition is around 10 KHz. We also detect the capacitor speed by applying a square voltage pulse, and measure the charging current of the device through a read resistor ($R_{\text{read}}=1$ KΩ, inset of Fig. 3). Since the charging or discharging time is dominated by the RC time constant, and R_{read} is much smaller than the device resistance, R can be replaced by R_{read}. Hence, we can approximately derive the device capacitance from the time-dependent charging current. Since the capacitance C may be time dependent in the transient response to the applied voltage pulse, we can cut the 50 μs charging window into several parts (0–2, 2–4, 4–10, and 10–50 μs). In each part, the capacitance of the device can be taken as a constant, so that we can use the equation, $I=I_a \exp(-t/RC)+I_o$, to fit the charging current in each part and find out the corresponding capacitance $C(t)$. By fitting the time-dependent charging current in various time ranges of the inset of Fig. 3, it was found that the capacitance of the capacitors is very small within 2 μs after applying the 2.6 V voltage pulse. The capacitance then increases quickly with time until it reaches the time range of 10–50 μs where the capacitance reaches an almost stable value (35 μF/cm^2, Fig. 3).

From this analysis, we found that our capacitors show a very large specific capacitance, which has a strong dependence on the relative humidity and nearly no dependence on LiF-layer thickness. AFM images (not shown here) show that the surface of both the Cu and LiF film have a nanocluster structure. The rms roughnesses of the LiF film are about 2.9 nm and 2.7 nm for the Cu film surface. Comparing with high surface carbon electrodes,[1] the Cu-electrode surface of our supercapacitor is not high. By increasing the surface area of the electrodes, we anticipate higher specific capacitance for our devices.

We proposed a double-layer model for explaining the anomalous capacitance in Cu/LiF/Cu system, as shown in Fig. 4. Since LiF has a certain solubility in water (0.1%, at room temperature),[16] when moisture is absorbed in the LiF film, a small amount of LiF is dissolved into lithium cations and fluoride anions. Under bias, the lithium cations will

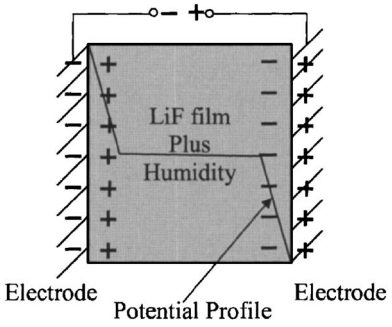

FIG. 4. The schematic diagram showing the capacitor's working principle.

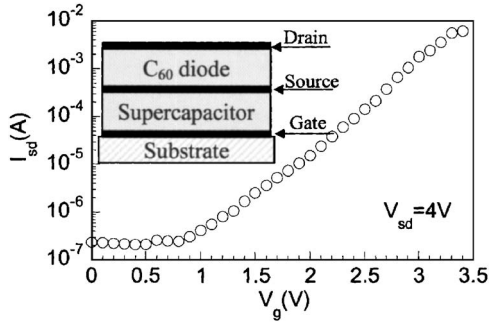

FIG. 5. The typical gate voltage dependence of the source-drain current, where the transistor shows low working voltage and high current output.

move along the applied external electric field direction and accumulate at the cathode/LiF interface on one hand. On the other hand, fluoride anions will move against the direction of the applied electric field and accumulate at the anode/LiF interface. As a result, positive charges and negative charges are accumulated on the anode and cathode plate, respectively. Hence, a double-layer supercapacitor is formed, which is the same principle as traditional electrochemical supercapacitors.[1] Most of the potential applied drops across the double-layer interfaces, and the double-layer charges provide a huge capacitance. Therefore, both the capacitance and the resistance of the device show very weak relation with the LiF thickness.

The beauty of our supercapacitor is that the fabrication processing is performed by only vacuum thermal evaporation methods. Therefore, it is easy to stack the supercapacitors vertically to form a multilayer case for enhanced capacitance. We have fabricated a six-cell Cu/LiF/Cu device with the cathodes and anodes of each cell connected, respectively. The specific capacitance of the device reaches as high as 205 μF/cm^2 at 25 Hz, 2 V dc bias and 50% RH condition (not shown here).

Another fascinating aspect of our supercapacitor is that it can be easily incorporated with other electronic devices, showing interesting electrical or optical characteristics and performance. One example is that when the supercapacitor was incorporated with an organic diode, a vertical organic field-effect transistor was formed (inset of Fig. 5). The middle electrode, shared by the supercapacitor cell and the organic cell, is defined as the source electrode, the other electrode of the supercapacitor is defined as the gate electrode, and the remaining diode electrode is defined as the drain electrode. With a very thin and rough source electrode we have built uniquely structured high-performance organic transistors.[14] Figure 5 shows the typical gate voltage dependence of the source-drain current, where the transistor shows low working voltage and high current output. Because of the thin and rough source electrode layer, there will be a remnant electric field at the source/organic interface when the capacitor cell is biased, which basically makes the transistor work. It should be mentioned that this supercapacitor works under humidity condition, while water may cause most organic electronic devices degradation. This issue may be solved by building in some water inside the ionic compound layer, so that the whole device can work under nonhumid environment. Details about this study are under investigation.

In summary, we have demonstrated an all-solid-state supercapacitor with the structure of metal/LiF/metal, which can be easily fabricated in one procedure by vacuum thermal evaporation methods. The supercapacitors showed specific capacitance up to tens of μF/cm^2, and relatively fast speed in the 10 kHz range. Experimentally, it was found that the device capacitance was almost LiF-thickness independent and showed a strong dependence on humidity. A double-layer model of an electrochemical capacitor is illustrated to explain the device working principle. The fabrication of the supercapacitor is similar to that of organic electronic devices. As a result, the supercapacitor can be used as a building block and be easily incorporated with other electronic devices or circuits. This opens a way for electronic device applications, especially organic electronic devices.

This work is supported by a research grant from the US Air Force Office of Scientific Research, Program Director Dr. Charles Lee. We would like to thank Dr. David Margolese for his help.

[1] B. E. Conway, *Electrochemical Supercapacitors: Scientific Fundamentals and Technological Application* (Kluwer Academic/Plenum, Dordrecht, 1999).
[2] M. G. H. M. Hendriks, M. J. G. W. Heijman, W. E. van Zyl, and J. E. ten Elshof, H. Verweij, J. Appl. Phys. **90**, 5303 (2001).
[3] J. Y. Kim and I. J. Chung, J. Electrochem. Soc. **149**, A1376 (2002).
[4] P. Gómez-Romero, M. Chojak, K. Cuentas-Gallegos, J. A. Asensio, P. J. Kulesza, N. Casañ-Pastor, and M. Lira-Cantú, Electrochem. Commun. **5**, 149 (2003).
[5] F. Lufrani and P. Staiti, Electrochim. Acta **49**, 2683 (2004).
[6] Y. Kibi, T. Saito, M. Kurata, J. Tabuchi, and A. Ochi, J. Power Sources **60**, 219 (1996).
[7] H. Nagawa, A. Shudo, and K. Miura, J. Electrochem. Soc. **147**, 38 (2000).
[8] S. T. Mayer, R. W. Pekala, and J. L. Kaschmitter, J. Electrochem. Soc. **140**, 446 (1993).
[9] E. Frackowiak, K. Metenier, V. Bertagna, and F. Beguish, Appl. Phys. Lett. **77**, 2421 (2000).
[10] M. Endo, Y. J. Kim, K. Osawa, K. Ishii, T. Inoue, T. Nomura, N. Miyashita, and M. S. Dresselhaus, Electrochem. Solid-State Lett. **6**, A23 (2003).
[11] L. Ma, J. Ouyang, and Y. Yang, Appl. Phys. Lett. **84**, 4786 (2004).
[12] J. H. Burroughes, D. D. C. Bradley, A. R. Brown, R. N. Marks, K. Mackay, R. H. Friend, P. L. Burn, and A. B. Holmes, Nature (London) **347**, 539 (1990).
[13] L. P. Ma, Q. F. Xu, and Y. Yang, Appl. Phys. Lett. **84**, 4908 (2004); L. P. Ma, S. M. Pyo, and Y. Yang, *ibid.* **82**, 1419 (2003); L. P. Ma, J. Liu, S. M. Pyo, and Y. Yang, *ibid.* **80**, 362 (2002); L. P. Ma, J. Liu, and Y. Yang, *ibid.* **86**, 2997 (2002); L. P. Ma, J. Liu, S. M. Pyo, Q. F. Xu, and Y. Yang, Mol. Cryst. Liq. Cryst. **378**, 185 (2002).
[14] L. P. Ma and Y. Yang, Appl. Phys. Lett. **85**, 5084 (2004).
[15] S. D. Wang, M. K. Fung, S. L. Lai, S. W. Tong, C. S. Lee, S. T. Lee, H. J. Zhang, and S. N. Bao, J. Appl. Phys. **94**, 169 (2003).
[16] *Handbook of Chemistry and Physics*, edited by R. C. Weast (CRC Press, Cleveland, 1964), p. B-187.